

per are presented in Table 1. These results show that twelve samples fall within the defined compositional limits of native copper from the Lake Superior area. The McClure Site sample is anomalous because of the relatively large quantities of lead, tin, and zinc, and a trace of nickel. However, it cannot be definitely stated at this time that it is not native copper (5). It should also be noted that our test results agree very closely with those previously conducted on copper artifacts from archeological sites in Iowa (4).

Within the limits of our research and laboratory techniques, we feel that we have shown that native copper artifacts occur in various archeological contexts dating between A.D. 700 and A.D. 1650 in the Dakotas, and that these artifacts were manufactured from ore

obtained in the Lake Superior area. Anthropological implications of trade and diffusion, as well as more refined laboratory analyses, need further research and collaboration.

WALTER E. HILL, JR.
State Geological Survey,
Lawrence, Kansas

ROBERT W. NEUMAN
Smithsonian Institution,
Lincoln, Nebraska

References and Notes

1. R. B. Cumming, Jr., *Smithsonian Inst. Bull.* **169**, No. 10 (1958).
2. C. S. Smith and R. T. Grange, Jr., *ibid.*, No. 11.
3. F. H. H. Roberts, Jr., *Smithsonian Inst. Annu. Rep.* (1961).
4. M. M. Wedel, *Missouri Archaeologist* **21**, Nos. 2-4 (1959).
5. T. Bastian, *Anthropological Papers*, Museum of Anthropology, University of Michigan, No. 17 (1961).

5 August 1966

Lithology and Paleontology of the Reflective Layer Horizon A

Abstract. Cores recovered from horizon A are Late Cretaceous (Maestrichtian) in age and consist of alternating layers of calcareous turbidites and "red clay." The presence of red clay suggests that the water depth in this area during Cretaceous time was at least as great as at present—more than 5100 meters. A middle Cretaceous (Cenomanian) core consisting of interbedded sand and gravel and light-to-dark-gray lutite was taken in the same area from a layer stratigraphically below the horizon; the presence of hydrogen sulfide and iron sulfide may indicate anaerobic conditions that may be attributable to local ponding of sediment in Cenomanian time.

The geophysical evidence and the significance of the reflective layer horizon A has been discussed (1). We now report its lithology and the paleontologic evidence of its Cretaceous (Maestrichtian) age.

Eight Cretaceous cores have been recovered from the outcrop area (Fig. 1): seven are Maestrichtian and appeared to be outcrops of horizon A on the seismic-profile records (1). All Cretaceous cores were taken in water depths exceeding 5100 m (Table 1).

In general, the seven cores consist of red clay overlying alternating layers of turbidites and normal pelagic (red-clay) sediments. The turbidites range in thickness from less than 10 cm to more than 2 m; they usually show a typical graded bedding, with coarse-grained sand or gravel at the base of each cycle. In most cases, coarser fractions of the turbidites consist of shallow-water foraminifers, corals, gastropods, pelecypods, and fish bones. In two of the cores, volcanic ash occurs in some of the turbidites. Some turbidites in the cores are comprised al-

most entirely of clay-size particles composed largely of coccolith plates.

Core V 21-236 consists of a moderate-yellowish-brown to grayish-orange lutite overlying alternating layers of white calcilutite, fine-grained foraminiferal sand, and yellowish-gray lutite; the Cretaceous portion begins at 260 cm. Core V 21-237 consists of pale-yellowish-brown and grayish-brown lutite overlying a layer of laminated lutite and manganese oxide and alternating layers of light-olive-gray lutite and foraminiferal sands; the Cretaceous portion is believed to begin at a depth of 48 cm.

Core V 21-238 is composed of a dark-yellowish-brown, burrow-mottled lutite overlying alternating layers of turbidites and moderate-yellowish-brown lutite; the Cretaceous portion begins around 26 cm. Core 239 consists of a pale-brown and olive-to-dark-gray lutite and silty lutite overlying interbedded layers of sand, turbidites, and dark-brown lutite; the Cretaceous portion begins around 700 cm.

Core V 21-241 consists of a

moderate-to-dark-yellowish-brown lutite overlying alternating layers of foraminiferal sand and mostly brownish lutite containing many coccoliths and a few foraminifers; the Cretaceous portion begins at 340 cm. Core V 22-12 comprises a pale-brown-to-dusty-yellow silty lutite overlying an olive-gray lutite, dark-yellowish-brown lutite, and quartzose and calcareous silt. Core V 22-16 consists of a pale-to-moderate-yellowish-brown and gray lutite overlying interbedded layers of reddish-brown lutite and yellowish-gray-to-light-gray sand; the Cretaceous portion begins at 60 cm.

As we have mentioned, no fossils younger than Cretaceous have been found in the turbidite sections of the cores described; Foraminifera indicating Maestrichtian age are *Globotruncana calciformis* Vogler, *G. gagebini* Tirev, *G. gansseri* Bolli, and *G. stuarti stuartiformis* Dalbiez; other longer-ranging foraminifers include *Schackoina multispinata* (Cushman and Wicken-den), *Globotruncana fornicata* Plummer, *G. havanensis* Voorwijk, *G. nothi* (Bronniman and Brown), *Globigerinelloides aspera* (Ehrenberg), *Rugoglobigerina rugosa* (Plummer), *Planoglobulina glabrata* (Cushman), *Pseudotextularia elegans* (Rzehak), and *Racemiguembelina fructifera* (Egger).

Foraminifers indicating Cretaceous age are found not only in the turbidites but also, much less abundantly, in the normal pelagic sediment between the turbidites. Foraminifers found in the normal pelagic sediments are predominantly planktonic; their tests show evidence of corrosion, in contrast with the fresh appearance of foraminiferal tests found in the turbidites, indicating that they were deposited in place rather than being contaminants from the interbedded turbidites. The presence of these indicators in the pelagic sediment establishes the Maestrichtian age of these cores.

One other Cretaceous core (V 22-8) was taken from a layer that outcrops stratigraphically below horizon A on the seismic-profile records; it consists of medium-olive-gray-to-dark-gray lutite and silty lutite overlying interbedded carbonate sands and gravels, light-green-olive-gray lutite, and dark-greenish-gray-to-medium-dark-gray lutite. Iron sulfide is present in the medium-dark-gray layer, and the odor of hydrogen sulfide was noted in this layer when the core was opened.

The upper 90 cm of this core con-

tains Recent-Pleistocene planktonic foraminifers; foraminifers of Upper Cenomanian age occur lower. Forms indicative of this time include *Schackoina cenomana* (Schacko), *Hedbergella amabilis* Loeblich and Tappan, *H. tro-*

choidea (Gandolfi), *Praeglobotruncana delrioensis* (Plummer), *P. stephani* (Gandolfi), *Globigerinelloides carseyi* Bolli, Loeblich, and Tappan, *Rotalipora evoluta* Sigal, and *R. reicheli* (Mornod).

Twenty-two other cores taken in the area do not penetrate horizon A (Table 1); four are Miocene in age and the remainder, consisting mostly of red clay, are presumably Pleistocene. Core V 21-229 is made up of interbedded foraminiferal sand and lutite and pebbly layers; most of the pebbles are limestone and subround, and many have a thin coating of manganese oxide; the Miocene portion begins around 40 cm. The foraminiferal assemblage indicates an Upper-Middle Miocene (Tortonian) age, of which indicative forms are *Globigerina nepenthes* Todd, *Globigerinoides obliquus* Bolli, *Sphaeroidinellopsis seminulina* (Schwager), and *Globoquadrina altispira* (Cushman and Jarvis). Reworked Cretaceous and Eocene species also are present.

Core V 21-243 is composed of a pale-brown lutite overlying interbedded layers of foraminiferal sand and pale-olive lutites; pelecypod fragments also are present in the foraminiferal zone and a few pieces of angular limestone occur; the Miocene portion begins around 60 cm. The foraminiferal assemblage indicates a Lower Miocene (Burdigalian) age, of which indicative forms are *Globorotalia fohsi barisanensis* LeRoy, *G. mayeri* Cushman and Ellisor, *Globoquadrina dehiscens* (Chapman, Parr, and Collins), and *Sphaeroidinellopsis seminulina* (Schwager). The core also contains Cretaceous planktonic foraminifers and numerous Eocene shallow-water benthonic foraminifers.

Core V 22-10 contains a dark-yellowish-brown-to-grayish-orange lutite overlying a pale-olive foraminiferal sand and gravel. The foraminiferal assemblage indicates a Lower Miocene (Aquitanian) age; some reworked Eocene and Cretaceous (Maestrichtian) foraminifers also are present. Foraminifera indicating the Aquitanian are *Globigerinoides bisphericus* Todd, *G. curva* Blow, and *Globorotalia fohsi barisanensis* LeRoy; some larger benthonic foraminifers such as *Lepidocyclina* spp., *Operculina* spp., and *Mio-gypsina* spp. also occur.

Core V 22-11 consists of dark-yellowish-brown-to-light-olive-gray lutite overlying interbedded layers of coarse-grained sand, sandy lutite, and foraminiferal sand. An Upper-Middle Miocene (Tortonian) age is indicated by the presence of planktonic foraminifers such as *Globigerina nepenthes* Todd, *Globigerinoides obliquus* Bolli,

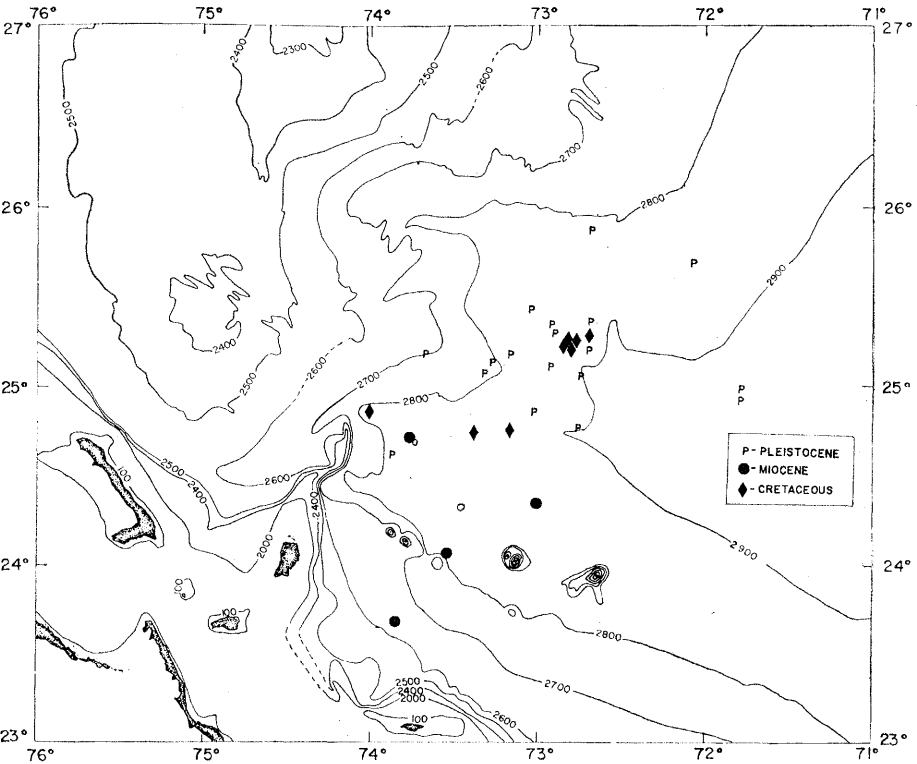


Fig. 1. Ages of cores from the area of the outcrop of horizon A.

Table 1. Sources and ages of cores taken from the area of the outcrop of horizon A.

Cruise	Core				
	No.	Source coordinates (N, W)	Water depth (m)	Length (cm)	Age
SHL 80	4	25°40.5', 72°05'	5214	370	Pleistocene
SHL 80	5	25°11.4', 72°42.5'	5258	278	Pleistocene
SHL 80	6	25°52', 72°41'	5134	91	Pleistocene
V 7	21	24°59', 71°48'	5495	80	Pleistocene
V 18	4	24°55', 71°47'	5320	430	Pleistocene
V 21	9	25°21', 72°41.5'	5376	605	Pleistocene
V 21	10	25°04', 73°20'	5084	1261	Pleistocene
V 21	11	25°11', 73°40'	4925	1240	Pleistocene
V 21	229	23°40', 73°51'	4782	399	M. Miocene
V 21	230	24°51', 73°02'	5245	917	Pleistocene
V 21	231	25°07', 73°17'	5095	1010	Pleistocene
V 21	232	25°10', 73°10'	5167	804	Pleistocene
V 21	233	25°25', 73°03'	5228	1068	Pleistocene
V 21	234	25°20', 72°56'	5249	1150	Pleistocene
V 21	235	25°18', 72°55'	5258	1010	Pleistocene
V 21	236	25°15', 72°47'	5282	744	Cretaceous
V 21	237	25°16', 72°42'	5276	855	Cretaceous
V 21	238	25°14', 72°48'	5286	401	Cretaceous
V 21	239	25°12', 72°51'	5278	1010	Cretaceous
V 21	240	25°06', 72°56'	5256	1039	Pleistocene
V 21	241	25°15', 72°50'	5278	1028	Cretaceous
V 21	242	25°03', 72°45'	5300	1510	Pleistocene
V 21	243	24°21', 73°01'	2564	426	L. Miocene
V 22	8	24°52', 74°01'	5329	487	Cretaceous
V 22	9	24°37', 73°53'	5112	1000	Pleistocene
V 22	10	24°43', 73°46'	5130	900	L. Miocene
V 22	11	24°03', 73°33'	5158	834	M. Miocene
V 22	12	24°45', 73°10'	5244	366	Cretaceous
V 22	14	24°45', 72°45'	5298	935	Pleistocene
V 22	16	24°44', 73°23'	5187	400	Cretaceous

Globoquadrina altispira (Cushman and Jarvis), *Globorotalia miotumida* Jenkins, and *Sphaeroidinellopsis seminulina* (Schwager); a few reworked Eocene and Cretaceous (Maestrichtian) foraminifers also are present.

One common characteristic of these

four Miocene cores is the presence of reworked specimens of *Pararotalia mexicana mecatepecensis* (Nuttall), an Eocene-Oligocene shallow-water benthonic foraminifer. The distribution of the Lower Miocene cores (Fig. 1) and their similar lithologies suggest that they

spread northward from a southerly source. This blanket of Miocene sediment masks horizon A in part of the outcrop area.

The lithology of the Pleistocene cores in this area is essentially a light-to-pale-yellowish-brown lutite (so-called

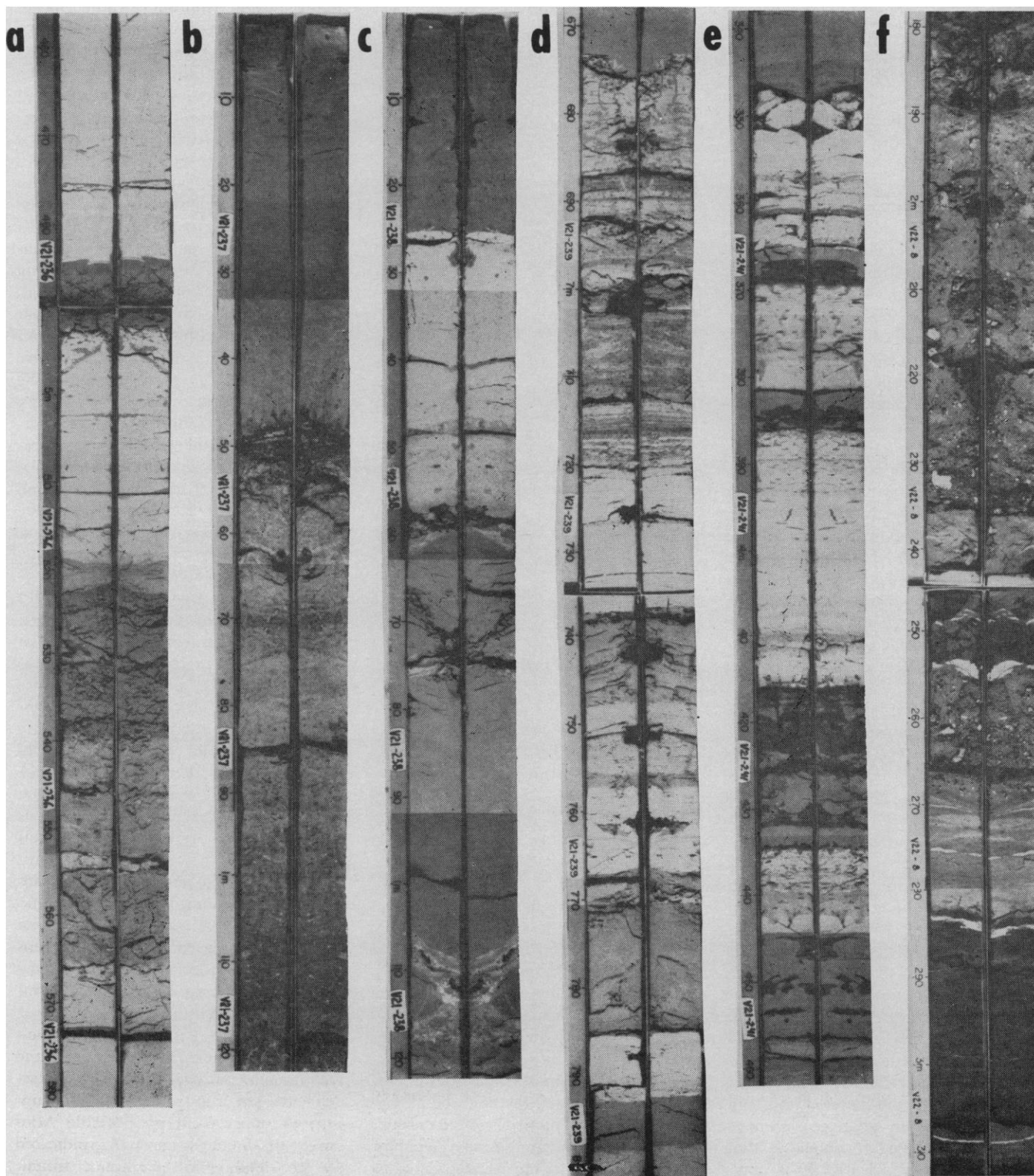


Fig. 2. Cretaceous cores recovered from horizon A: (a) V21-236; (b) V21-237; (c) V21-238; (d) V21-239; (e) V21-241; (f) V22-8 (taken from a stratigraphically lower layer). See text for lithologic descriptions.

red clay), with occasional turbidites of sand; most contain a few foraminifers and coccoliths of Pleistocene or Recent age. Their lithology establishes the Recent and Pleistocene sedimentary regime in this area and is further evidence that the Cretaceous cores came from a unique outcrop.

To our knowledge this is the first report of Cretaceous red clays that are definitely deep-sea in origin, a fact of particular importance in the history of the Atlantic. Results of emission spectrochemical analysis suggest that deep oceanic clay can be distinguished from normal shales on the basis of the manganese content (2). Normal shales contain 300 to 850 ppm Mn whereas oceanic clays contain 4000 to 9180 ppm. A sample of red clay from a depth of 790 cm in core V 21-241 contains 5500 ppm Mn, a content similar to that of deep clays under the modern oceans (3). Presence of the red clay in the Cretaceous cores indicates that sediments were deposited below the carbonate compensation depth and suggests that the Cretaceous sea in this part of the Atlantic was at least as deep as at present.

We should also point out that, according to an interpretation of the seismic-profile records, the area of the horizon A outcrop was uplifted to its present depth (1). Thus it is possible that the depth of the water at the time of deposition of horizon A was greater than at present. Those who believe that the Atlantic Ocean basin is a geologically young feature must consider this point.

The exposure of abyssal Cretaceous sediments here must be partly attributed to erosion (1); the mixed faunas reported in several cores are additional evidence of this. The abundance of turbidites in the Cretaceous deposits reinforces the earlier suggestion that these beds were level, or nearly so, when deposited, so that major irregularities in the topography of horizon A probably result from postdepositional deformation. The exposure of horizon β appears to be more closely associated with regional uplift.

The presence of iron sulfide and the odor of hydrogen sulfide in core V 22-8 may demonstrate anaerobic conditions near the sediment-water interface in Cenomanian time at this site. Such conditions in younger sediments have been attributed to either ponding of stagnant bottom water by a topographic barrier (4) or depletion of oxygen by overabundance of organic sub-

stance (5). However, Emery (6) has pointed out that both hydrogen sulfide and iron sulfide can form in sediments beneath aerobic waters, but that the interstitial waters, because of their slow circulation, can become anaerobic. At present, the few seismic-profile records from this area show some evidence of sediment ponding during Cenomanian time.

TSUNEMASA SAITO

LLOYD H. BURCKLE

MAURICE EWING

Lamont Geological Observatory,

Columbia University,

Palisades, New York

References and Notes

1. J. I. Ewing, J. L. Worzel, M. Ewing, C. Windisch, *Science*, this issue.
2. S. K. el Wakeel and J. P. Riley, *Geochim. Cosmochim. Acta* **25**, 110 (1961); K. M. Horn and J. A. S. Adams, *ibid.* **30**, 279 (1966).
3. A chemical, mineralogic, and petrographic study of the sample was made by H. M. Dahl and W. L. Hall at Bellaire Research Laboratories of Texaco, Inc.
4. R. H. Fleming and R. Revelle, in *Recent Marine Sediments*, P. D. Trask, Ed. (Soc. Econ. Paleontologists Mineralogists Spec. Publ. **4**, 1955), p. 96.
5. K. M. Ström, *ibid.*, p. 356.
6. K. O. Emery, in *Habitat of Oil*, L. G. Weeks, Ed. (Amer. Assoc. Petroleum Geologists, Tulsa, Okla., 1958), p. 965.
7. Supported by ONR contract Nonr 266 (48) and NSF grant GA 558. We are greatly indebted to F. D. Bode, H. M. Dahl, and W. L. Hall of Bellaire Research Laboratories of Texaco, Inc. We also thank J. I. Ewing, C. Windisch, and X. Le Pichon for reviewing and discussing the manuscript. Figure 1 was drawn by P. Buhl. Lamont Geological Observatory contribution No. 997.

17 August 1966

Melting of Tin Telluride at High Pressures

Abstract. *The melting curve of tin telluride ($\text{Sn}_{0.496}\text{Te}_{0.504}$) was determined by differential thermal analysis at pressures between 5 and 40 kilobars. Near $844^\circ \pm 4^\circ\text{C}$ and 12.0 ± 1.0 kb, the liquid and two solid polymorphs coexist.*

The compounds of elements of groups IV and VI, GeS, GeSe, GeTe, SnS, SnSe, SnTe, PbS, PbSe, PbTe, a technologically interesting group of materials, are chemically and structurally related to each other and to the group V elements P, As, Sb, Bi. Recent high-pressure investigations (1) have suggested further simple and useful correlations for phase relations of chemically and structurally related groups of elements and compounds. We now report determination of the melting curve of SnTe at pressures up to 40 kb; we have correlated some of

the data for phase relations of the group IV-group VI compounds.

Differential thermal analysis techniques (2) in piston-cylinder apparatus were used to observe meltings and freezings at elevated pressures. Freshly powdered samples (3) of $\text{Sn}_{0.496}\text{Te}_{0.504}$ contained in tantalum (two runs) and molybdenum capsules sealed (4) with Pyrex, were run in previously described furnace assemblies (5). Chromel-alumel thermocouples, typically about 0.3 mm from the sample, measured temperature; we attempted no corrections for the effects of pressure on thermocouple emf.

Results for the melting of SnTe are shown in Fig. 1. Heating signals were taken for the phase boundary in the Mo and Ta (1st) runs; for the Ta (2nd) run, cooling signals were considerably more distinct than heating signals. The overall precision in temperature appears to be within about 3°C (Fig. 1), although precision and reproducibility in a given run were within about 1° or 2°C . Friction corrections (2) were made by averaging compression and decompression pressures for the same transition temperature, with typical "single-values" of friction being 1.9 kb near 20 kb and 2.5 kb near 40 kb. Overall accuracy for pressure appears to be within about 1.0 kb.

A liquid-solid-solid triple point occurs near $844^\circ \pm 4^\circ\text{C}$ and 12.0 ± 1.0 kb (Fig. 1). No temperature-induced solid-solid transitions are known at zero pressure for the *BI* (rocksalt) structure in SnTe, and no signals were observed in our high-temperature, high-pressure explorations within stability fields of the solid phases. The structure of the solid melting below 12 kb is therefore presumed to be *BI*; above 12 kb, the phase that melts is apparently that reported by Kafalas and Mariano (6) as being stable above 18 kb at room temperature. The solid-solid phase boundary, which we could not detect, is drawn from the triple point toward the room temperature 18 kb coordinate (dotted line in Fig. 1).

Near zero pressure, the $\text{Sn}_{0.496}\text{Te}_{0.504}$ compound melts congruently at $805.9^\circ \pm 0.3^\circ\text{C}$ (7). With increasing pressure, the melting possibly becomes incongruent; our experiments could not delineate any such effect but did suggest an upper limit of $\sim 5^\circ\text{C}$ to any range of incongruent melting below 40 kb. Difficulties (2) in obtaining data below ~ 5 kb preclude accurate determination of the initial melting